

Experimental Measurements of Multipath-Induced Intra- and Inter-Channel Crosstalk Effects in a Millimeter-Wave Communications Link using Orbital-Angular-Momentum Multiplexing

Yan Yan¹, Long Li¹, Guodong Xie¹, Changjing Bao¹, Peicheng Liao¹, Hao Huang¹, Yongxiong Ren¹, Nisar Ahmed¹, Zhe Zhao¹, Martin P. Lavery², Nima Ashrafi^{3,4}, Solyman Ashrafi³, Dr. Shilpa Talwar⁵, Soji Sajuyigbe⁵, Moshe Tur⁶, Andreas F. Molisch¹, and Alan E. Willner¹

1. Department of Electrical Engineering, University of Southern California, Los Angeles, CA 90089, USA.

2. University of Glasgow, Glasgow, G12 8QQ, UK

3. NxGen Partners, Dallas, TX 75219, USA

4. University of Texas at Dallas, Richardson, TX 75080, USA

5. Intel Labs, Intel Corporation, Santa Clara, USA

6. School of Electrical Engineering, Tel Aviv University, Ramat Aviv 69978, ISRAEL.

Corresponding email*: yanyan@usc.edu

Abstract—This paper reports on an experimental measurement and analysis of multipath-induced intra- and inter-channel crosstalk effects in a mm-wave communications link using orbital angular momentum multiplexing at 28 GHz. The reflection is from an ideal reflector parallel to the propagation path. The intra-channel crosstalk effect is measured when a single OAM beam is transmitted, and inter-channel crosstalk effect is measured when 2 multiplexed OAM beams are transmitted. Both simulation and experimental results show that OAM channels with larger OAM number ℓ tend to have stronger intra-channel crosstalk because less power is received from the direct path and more power is received from the reflected path. This effect is caused by OAM beam divergence, as OAM beams with larger ℓ spread into a larger beam size and have less power in the beam center. For the same reason, OAM beams of larger ℓ lead to stronger inter-channel crosstalk with the other OAM channels.

Keywords—Multipath effect; millimeter wave; Orbital angular momentum; Spatial-division multiplexing.

I. INTRODUCTION

There is always a desire for higher capacity of point-to-point free-space communications links for various applications, including backhaul and data centers [1,2]. One approach to increase the total capacity in a link is to transmit multiple independent data streams over the same physical medium. Orthogonality among different data streams helps enable the efficient multiplexing and demultiplexing at the transmitter and the receiver, respectively [3]. If the multiplexed streams propagate along the same axis, they use only a single aperture at the transmitter and a single aperture at the receiver, i.e., a single aperture pair. One method to implement such multiplexing, which has received great interest recently, is orbital-angular-momentum (OAM) [4,5] multiplexing. OAM characterizes an electromagnetic wave with a phase front that “twists” in a helical fashion as it propagates. There exists a series of OAM twisting values (phase shifts) that are integer multiples of 2π , which represent an orthogonal basis set. The

phase term of the wavefront of OAM beams is described as $\exp(i\ell\phi)$, where ℓ is an integer values known as the OAM state value. There are several previously reported results of OAM multiplexing in both optical and RF communications [6-8]. Recently, we have demonstrated millimeter-wave OAM multiplexing, achieving 32-Gbit/s transmission using 8 independent OAM beams (4 OAM beams on each of 2 polarizations) without the need for electronic digital signal processing to cancel the channel interference thanks to the inherent orthogonality and low crosstalk among the beams [9].

As in all wireless communications systems, multipath effects can have important effects on OAM multiplexing systems. Some of those effects are similar to the case of conventional RF free-space links. However, there are several unique factors in an OAM-multiplexed link that present interesting technical challenges:

- (1) **Intra- and inter-channel crosstalk**: Energy can be coupled not only into the same data channel of the same OAM value (i.e., as in a conventional single beam link) but also into another data channel of a different OAM value. Therefore, both intra- and inter-channel crosstalk can occur.
- (2) **The beam intensity and phase**: An OAM beam has a “doughnut” intensity profile that has little power in the center and a power maximum around a ring, and the beam has a circular phase change with values that are integer multiples of 2π , depending on the OAM value ℓ . Importantly, the angle of the multipath reflection will determine into which OAM mode the reflected power will couple. Moreover, higher-order OAM beams diverge into a larger beam size.

Contributions: In this paper, we experimentally measure the multipath-induced intra- and inter-channel crosstalk effects caused by the reflection from a metal reflector in an mm-wave communications link which is based on OAM multiplexing. We show how the beam divergence and distorted helical phase

structure caused by reflection result in multipath-induced intra- channel and inter-channel crosstalk. Both experimental and simulation results show that OAM channels with larger OAM state number ℓ tend to have stronger intra-channel crosstalk because less power is received from the direct path and more power is received from the reflected path. This effect is mainly due to the fact that OAM beams with larger ℓ spread into a larger beam size and have less power in the center. For the same reason, OAM beams with larger ℓ cause stronger inter-channel crosstalk with the other OAM channels.

II. MULTIPATH EFFECT OF OAM CHANNELS

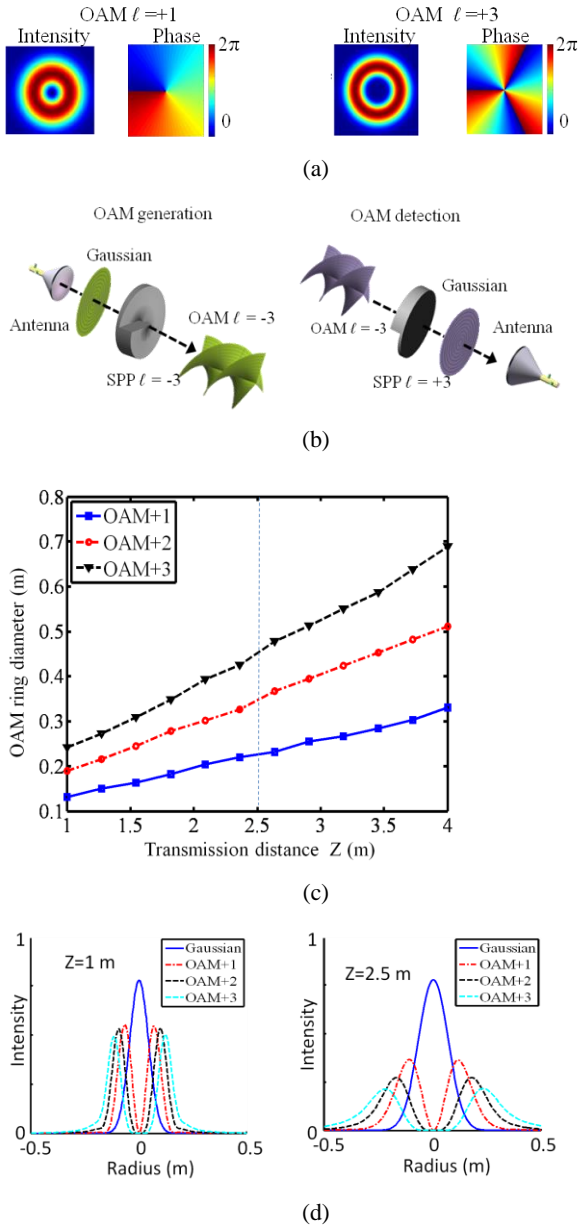


Figure 1. (a) Ring-shaped intensity and helical wavefront phase of OAM beams with $\ell=+1$ and $\ell=+3$. (b) Generation and detection of OAM beams using lensed horn antennae and spiral phase plates (SPPs). (c) The ring diameters of the OAM beams' intensity with different ℓ as functions of propagation distance. (d) The beam profile

of a Gaussian beam and OAM beams at transmission distances of 1 m and 2.5 m.

Figure 1 shows the generation, detection, and propagation of OAM beams. Fig. 1(a) shows that OAM beams have a ring-shaped intensity profile and a helical wavefront phase $\varphi(\theta)=\ell\theta$, in which $0<\theta<2\pi$ is an azimuthal angle and ℓ is an integer known as the OAM state number. Fig. 1(b) shows that an OAM beam can be generated by passing a Gaussian beam through a spiral phase plate (SPP) of which the thickness increases azimuthally [9]. To detect an OAM beam, an SPP with the opposite OAM number $-\ell$ is used to convert the OAM beam back into a Gaussian beam and then detected by an antenna. Due to the helical wavefront phase $\varphi(\theta)=\ell\theta$, OAM beams with different ℓ are spatially orthogonal to each other when they propagate coaxially. OAM beams diverge as they propagate. Fig. 1(c) shows the beam divergence of the OAM beams. The simulated results show the ring diameters of the OAM beams intensity with different ℓ as functions of propagation distance as the Gaussian beam diameter before the SPP is 7.5 cm and the mm-wave frequency is 28 GHz. Fig. 1 (d) shows one-dimensional intensity profiles of the OAM beams at two transmission distances. One can see that higher-order OAM beams diverge into larger sized beams and have less power in their center.

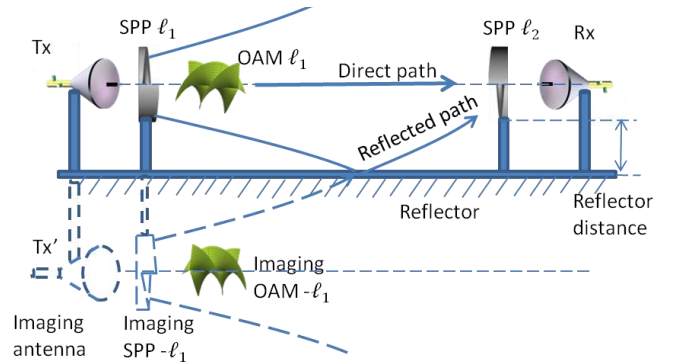


Figure 2. Multipath effects of an OAM channel caused by the specular reflection from the ground, which is considered as an ideal reflector here. Due to the beam divergence, part of the OAM beam will be reflected. The reflected OAM beam can be treated as an off-axis OAM beam from the imaging antenna Tx' and the imaging SPP'.

The simulation results in Fig. 3 show an example of the intra-channel and inter-channel crosstalk from the reflected path. The left column shows the intensity, phase, and OAM spectrum of the direct OAM beam with $\ell_1=+3$ from the direct path. Ideally due to the spiral phase structure, all the power will be in the OAM state of $\ell_1=+3$. The middle column shows the reflected OAM beam, which can be considered as being generated by the imaging antenna and the imaging SPP in Fig. 2. Although still having a spiral phase and ring-shaped intensity, the reflected OAM beam is offset to the direct path axis and is not coaxial with the OAM beams in the direct path, and so that is no longer spatially orthogonal to the OAM beams in the direct path [11]. When the reflected OAM beam is decomposed at the receiver with respect to the OAM basis along the direct path axis, the beam power is spread onto a wide range of OAM states ℓ , which leads to intra-channel crosstalk with the OAM channel $\ell_1=+3$ and inter-channel

crosstalk with the other OAM channels. The right column in Fig. 3 shows the actual beam at the receiver, which is the superposition of the direct OAM and the reflected OAM. The intensity has a clear fringing pattern due to the interference between the direct beam and the reflected beam. The phase is also distorted due to the multipath effect. The overall OAM spectrum of the beam at the receiver is also spread over a range of OAM states because of the inter-channel crosstalk, and the power in the OAM state ℓ_1 is different from the one in the direct path because of the intra-channel crosstalk.

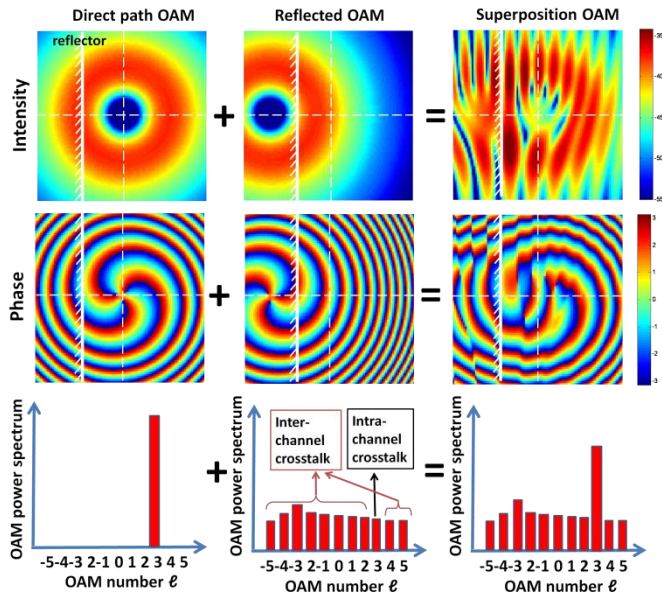
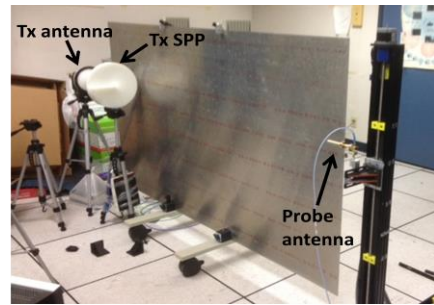


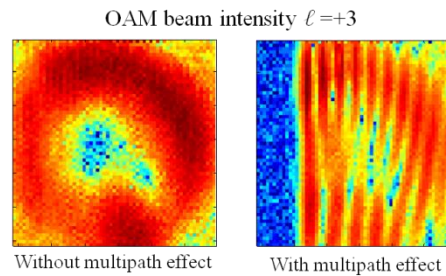
Figure 3. Illustrations of intensity, phase, and OAM spectrum of the direct path OAM beam, reflected path OAM beam, and the actual beam at the receiver. The actual beam is the superposition of the direct OAM and the reflected OAM. Since the reflected OAM beam is off-axis, it is no longer orthogonal to the OAM beams in the direct path and will cause both inter-channel and intra-channel crosstalk. The white solid line represents the reflector.

Fig. 4(a) shows the experimental setup for investigating the multipath effects of OAM channels. A lensed horn antenna and a spiral plate are used to generate a mm-wave OAM beam at 28 GHz. A planar aluminum sheet (2.5 m long \times 1.5 m height) is mounted on a cart and placed parallel to the propagation path. The distance between the path and the reflector can be changed by moving the cart. As the distance between the path and reflector decreases, the multipath effect becomes stronger. As an example, Fig. 4 (b) shows the intensity of an OAM beam with $\ell=+3$ when there is no reflector, while Fig. 4 (c) shows the intensity when the reflector is placed close to the propagation path. The intensity of the mm-wave beam is acquired by scanning a probe antenna in the transverse plane at the receiver side [9]. There is a fringe pattern caused by the interference between the direct beam and the reflected beam. In the experiment, the propagation distance between the Tx SPP and Rx SPP is 2.5 m. The diameter of the lensed horn antenna is 15 cm. The diameter of the SPPs to generate and detect OAM channels is 30 cm. We refer to the SPPs at the transmitter (Tx) and the receiver (Rx) as the Tx and Rx aperture, respectively. We use the imaged antenna model in Fig. 2 and the OAM

mode decomposition method [12] to analyze the multipath effects of the OAM channels.



(a)



(b)

(c)

Figure 4 (a) Experiment setup for investigating the multipath effects of OAM channels. A movable aluminum sheet is used as an ideal reflector, which is placed parallel to the propagation path. (b) The intensity of the OAM beam $\ell=+3$ without and (c) with the multipath effects.

III. MULTIPATH EFFECT ON A SINGLE OAM CHANNEL AND INTRACHANNEL CROSSTALK

First, we investigate the intra-channel crosstalk, i.e., the multipath effect of a single OAM channel, which means that at the Tx, only the OAM beam of $\ell = \ell_1$ is transmitted and at the Rx, only $\ell = \ell_1$ is received. Figure 5 shows the experimental results of the normalized received power at the Rx as a function of the reflector distance after demultiplexing for OAM beams of different ℓ . In the experiment, all OAM channels have the same transmitted power and a 28 GHz continuous-wave (CW) signal is used. We change the SPPs at both sides of the Tx and Rx to study the multipath effects for OAM beams with different ℓ values. Two effects are observed: First, the received power for OAM beams with a larger ℓ is lower, which is explained by the divergence property of OAM beams [12]. Second, when the reflector distance is small, the received power for the OAM channels varies as the reflector distance changes, which is explained by the interference between the signals from the direct and reflected paths [3]. Moreover, a stronger power fluctuation is observed for a larger ℓ , which indicates a stronger multipath effect for OAM channels of higher order.

To study the intra-channel crosstalk, we look into the reflected-to-direct power ratio of the OAM channels, which is defined as the ratio of the received power from the reflected path to the received power from the direct path.

$$\text{reflected-to-direct power ratios} = \frac{\text{Received reflected power}}{\text{Received direct path power}} \quad (1)$$

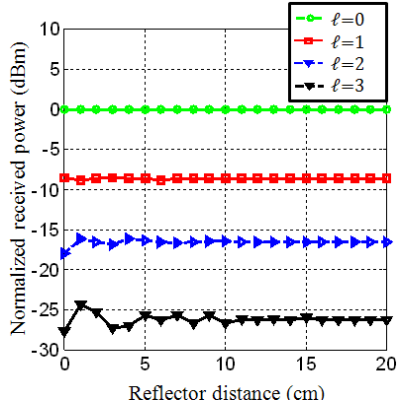


Figure 5. Experimental results of the received power after demultiplexing for different OAM beams as functions of the reflector distance.

Fig. 6 shows the simulated and measured reflected-to-direct power ratios as functions of the reflector distance for OAM channels with different ℓ . In the simulation, the received power of the direct path is calculated based on the beam emitted from the real antenna Tx after demultiplexing, and the power of the reflected path is calculated based on the beam from the imaging antenna Tx' after demultiplexing (see Fig. 2). In the experiment, we obtain the reflected-to-direct power ratio using a vector network analyzer (VNA). The VNA measures the complex amplitude of the total received signal as a vector \vec{v} . When there is no reflector, the received signal amplitude from the direct path is \vec{v}_d . We assume that the reflector does not affect the direct path signal as long as the distance between the reflector and the propagation axis is greater than the aperture radius. Then, the amplitude from the indirect path \vec{v}_r is:

$$\vec{v}_r = \vec{v} - \vec{v}_d \quad (2)$$

\vec{v} is the measured received signal when the reflector is at different distance. Then, we calculate the reflected signal using Eq. (2) and get the reflected-to-direct power ratio. Both

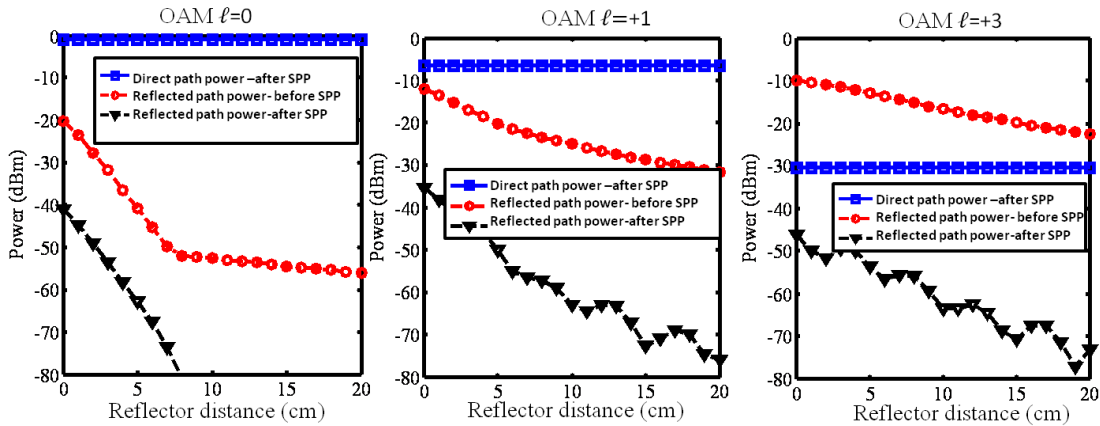


Figure 7. Analysis of intra-channel crosstalk for a Gaussian beam and OAM beams of $\ell=+1$ and $\ell=+3$ due to the multipath effects (Simulation results). Blue line: the received power from the direct path by the Rx antenna for a specific OAM channel after demultiplexing (after the Rx SPP). Red line: the total power collected by the Rx aperture from the reflected path before demultiplexing (before the Rx SPP). Black line: the received power from the reflection path by the Rx antenna for a specific OAM channel after demultiplexing (after the Rx SPP)

simulation and measurement results in Fig. 6 show that an OAM channel with a larger ℓ has a higher reflected-to-direct power ratio and has stronger intra-channel crosstalk.

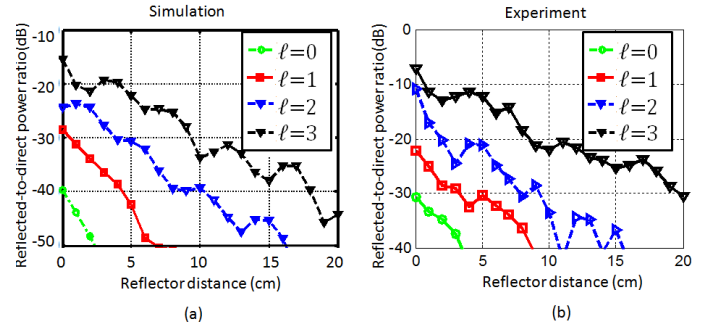


Figure 6. (a) Simulation and (b) experiment results of the reflected-to-direct power ratio for a Gaussian beam and different OAM beams.

The simulation results in Fig. 7 show a more detailed analysis of the intra-channel crosstalk of the Gaussian beam and OAM beams. The blue line shows the received power from the direct path by the Rx antenna for a specific OAM channel after demultiplexing (after Rx SPP). The power from the direct path decreases when the OAM number increases, which is explained by the divergence characteristics of OAM beams, as shown in Fig. 1. The red line shows the total power collected by the Rx aperture from the reflection path before demultiplexing (before the Rx SPP). The total power from the reflected path increases as the OAM number increases, because for a larger ℓ , the beam spreads and becomes larger so that more energy gets reflected. The black line shows the received power from the reflection path at the Rx antenna for a specific OAM channel after demultiplexing (after the Rx SPP). The difference between the total power and the received power from the reflected path is explained as follows: Due to its spiral phase structure, the Rx SPP acts like a spatial “filter” to extract the power of a specific OAM beam from all the energy collected by the Rx aperture, and only the energy in a specific OAM mode will be received by the Rx antenna. The trend

shown by the blue and red lines can be explained by the intensity properties of the OAM beams, while the difference between the red and black lines can be explained by the filter effect due to the spiral phase structure of the OAM beams. On the one hand, the beam divergence reduces the power from the direct path and increases the total reflected power as ℓ increases, resulting in stronger multipath effects. On the other hand, the phase structure of SPP helps increase the difference between the total reflected power and the actual received power from the reflected path (the difference between the red and black lines), which reduces the multipath effect for a larger ℓ . The overall intra-channel crosstalk is the difference between the black and blue lines, which increases as ℓ increases, indicating stronger intra-channel crosstalk for OAM beams with a larger ℓ .

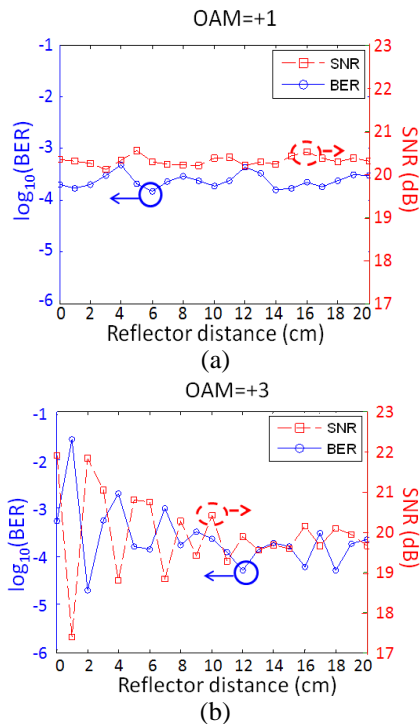


Figure 8. Measured BER and SNR as functions of the reflector distance for (a) $\ell=+1$ and (b) $\ell=+3$. A stronger fluctuation of BER and SNR is observed for OAM $\ell=+3$ because of the stronger intra-channel crosstalk induced by multipath effect.

Next, we transmit a 1-Gbaud 16-QAM signal on the OAM beams to determine how the multipath effects impact the OAM channels' performance. As shown in Figs. 5 and 6, significant multipath effects are observed when the distance between the reflector and the aperture is between 0 and 10 cm, corresponding to a difference in length between the direct and indirect paths of 1.7 cm~5 cm (a time delay of 55 ps~166 ps), which is estimated from the geometry in Fig. 2. Since the wavelength is 1.07 cm for a 28 GHz carrier frequency, SNR variations are due to the interference effects that depend on the reflector distance. The transmitted 1-Gbaud signal has a 1-ns symbol duration (30 cm symbol length in free space). Since the multipath delay is much smaller than the symbol duration, no significant inter-symbol interference (ISI) occurs [13]. Fig. 8 shows the BER and SNR as functions of the reflector distance

for OAM channels $\ell=+1$ and $\ell=+3$ when the 1-Gbaud 16-QAM signal is transmitted. For $\ell=+1$, since the intra-channel crosstalk is smaller, weaker SNR and BER variation are observed when the reflector distance changes. For OAM $\ell=+3$, stronger channel interference and much stronger fluctuations of SNR and BER are observed when the reflector distance changes. The results show that an OAM channel with a larger ℓ is more affected by intra-channel crosstalk.

IV. MULTIPATH EFFECT OF MULTIPLEXED OAM CHANNELS AND INTER-CHANNEL CROSSTALK

The multipath effect also introduces inter-channel crosstalk when multiple OAM channels are multiplexed. First we measure the inter-channel crosstalk when the Tx SPP OAM number ℓ_1 is fixed and the Rx SPP OAM number ℓ_2 takes different values to characterize how much power of OAM channel ℓ_1 is received by OAM channel ℓ_2 due to multipath effects. Fig. 9 shows the measurement of the inter-channel crosstalk as a function of the reflector distance when OAM channels with $\ell_1=+1$ and $\ell_1=+3$ are transmitted, respectively. When the reflector distance is large and the multipath effect is negligible, the difference between the received power of the transmitted OAM channel and the other OAM channels is large, which shows that there is negligible inter-channel crosstalk among the OAM channels. As the reflector distance decreases, the received power of the other OAM channels increases due to the stronger multipath effect. Similar to the inter-channel crosstalk, by comparing the results for $\ell_1=+1$ and $\ell_1=+3$ we see that the received power difference between the transmitted channel and the other OAM channels is small for a larger ℓ_1 value, which means that an OAM channel with a larger ℓ will have stronger inter-channel crosstalk with other channels.

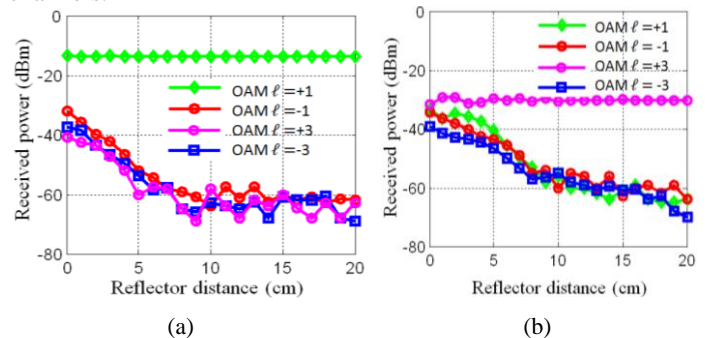


Figure 9. Measurement of inter-channel crosstalk when (a) $\ell=+1$ and (b) $\ell=+3$ is transmitted, respectively.

We then multiplex two OAM beams of $\ell=+1$ and $\ell=+3$, where each of them carries an independent 1-Gbaud 16-QAM data stream, and we change the reflector distance to investigate the system performance when both intra-channel and inter-channel crosstalk is caused by the multipath effects. In the multiplexing experiment, the received power for $\ell=+1$ and $\ell=+3$ is the same at the receiver antenna. Fig. 10(a) and (b) show the BER as a function of the reflector distance for $\ell=+1$ and $\ell=+3$ (the SNR for both channels is ~ 22 dB when there is no reflector). Comparing Fig. 10(a) with Fig. 8(a), the BER of OAM channel $\ell=+1$ is observed to significantly increase when there is inter-

channel crosstalk from OAM channel $\ell=+3$. For OAM channel $\ell=+3$, Fig. 10 (b) shows a similar BER variation as observed in Fig. 8 (b) because the degradation of OAM channel $\ell=+3$ is mainly caused by intra-channel crosstalk, and not much caused by the inter-channel crosstalk from OAM channel $\ell=+1$. Furthermore, we take the BER measurement as a function of SNR at different reflector distances, as shown in Fig. 11(a) and Fig. 11(b). Because OAM $\ell=+1$ receives a stronger inter-channel crosstalk signal from OAM $\ell=+3$, there is clearly an increasing power penalty as the reflector distance decreases. For OAM $\ell=+3$, there is a smaller power penalty difference for different reflector positions, indicating that OAM $\ell=+3$ receives much smaller inter-channel crosstalk from OAM $\ell=+1$

their center. For the same reason, OAM beams with a larger ℓ cause stronger inter-channel crosstalk with the other OAM channels. The investigation here concentrates on the fundamental effect of multipath, and thus considers a single specular reflector. This scenario is not only practically relevant as being similar to a ground reflection, but also provides insights into the interaction of direct and reflected components. Further work will investigate the joint impact of multiple reflectors.

ACKNOWLEDGMENT

This work is supported by the Intel Labs University Research Office and NxGen Partners. We are thankful for the fruitful discussion with Dr. David Ott.

REFERENCES

- [1] S. Hur, T. Kim, David J. Love, J. V. Krogmeie, Timothy A. Thomas and A. Ghosh, "Millimeter Wave Beamforming for Wireless Backhaul and Access in Small Cell Networks," *IEEE Transactions on Communications* vol. 61, no. 10, pp. 4391-4402, 2013
- [2] Y. Katayama, K. Takano, Y. Kohda, N. Ohba, and D. Nakano, "Wireless data center networking with steered-beam mmWave links," *IEEE Wireless Communications and Networking Conference 2011*, pp. 2179 - 2184
- [3] A. F. Molisch, *Wireless Communications* 2nd edn (Wiley, 2011)
- [4] L. Allen, M. W. Beijersbergen, R. J. C. Spreeuw, and J. P. Woerdman, "Orbital angular momentum of light and the transformation of Laguerre-Gaussian laser modes," *Physical Review A*, vol. 45, no. 11, pp. 8185-8189, 1992.
- [5] G. Gibson, J. Courtial, M. Padgett, M. Vasnetsov, V. Pas'ko, S. Barnett, and S. Franke-Arnold, "Free-space information transfer using light beams carrying orbital angular momentum," *Opt. Express*, vol. 12, pp. 5448-5456, 2004.
- [6] J. Wang, J.-Y. Yang, I. M. Fazal, N. Ahmed, Y. Yan, H. Huang, et. al., "Terabit free-space data transmission employing orbital angular momentum multiplexing," *Nature Photonics*, vol. 6, pp. 488-496, 2012.
- [7] F. Tamburini, E. Mari, A. Sponselli, B. Thidé, A. Bianchini, and F. Romanato, "Encoding many channels on the same frequency through radio vorticity: first experimental test," *New Journal of Physics*, vol. 14, no. 3, pp. 033001, 2012.
- [8] F. E. Mahmoudi, and D. Walker, "4-Gbps uncompressed video transmission over a 60-GHz orbital angular momentum wireless channel," *Wireless Communications Letters*, vol 2, no. 2, pp. 223-226, 2013.
- [9] Y. Yan, G. Xie, M. Lavery, H. Huang, N. Ahmed, et al., "High-capacity millimetre-wave communications with orbital angular momentum multiplexing," *Nature Communications* vol 5, pp. 4876 (2014)
- [10] S. H. Byun, G. A. Hajj, and L. E. Young, "Development and application of GPS signal multipath simulator," *Radio Science*, vol 37, no.6, pp. 1098, 2002.
- [11] Y. Ren, L. Li, G. Xie, Y. Yan, Y. Cao, et al., "Experimental demonstration of 16 Gbit/s millimeter-wave communications using MIMO processing of 2 OAM modes on each of two transmitter/receiver antenna apertures," accepted to *IEEE Global Telecommunications Conference 2014*.
- [12] G. Xie, L. Li, Y. Ren, H. Huang, Y. Yan et al., "Performance Metrics and Design Parameters for a Free-space Communication Link Based on Multiplexing of Multiple Orbital-Angular-Momentum Beams," accepted to *IEEE Global Telecommunications Conference 2014*.
- [13] J. G. Proakis and M. Salehi, *Digital Communications*, 5th edn (McGraw-Hill 2007)

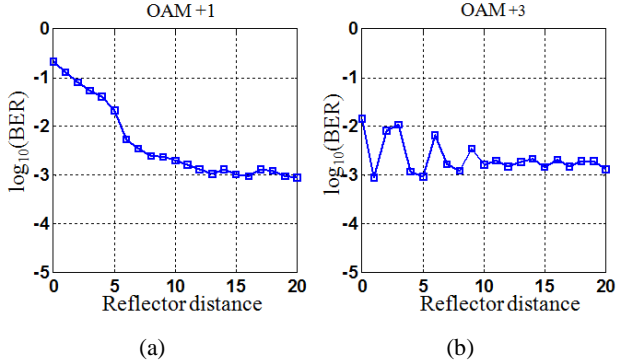


Figure 10. Measurement of BER as a function of the reflector distance when (a) $\ell=+1$ and (b) $\ell=+3$ (b) is received when $\ell=+1$ and $\ell=+3$ are multiplexed.

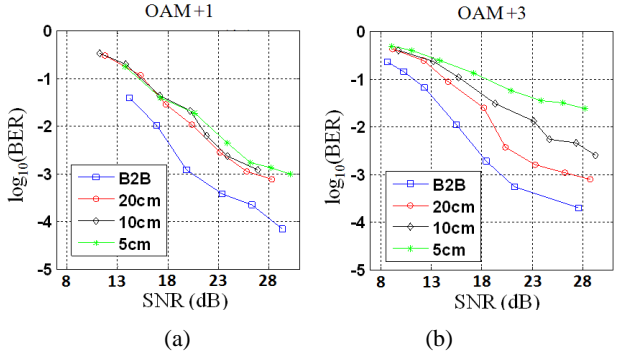


Figure 11. Measured BER as a function of SNR for (a) $\ell=+1$ and (b) $\ell=+3$ (b) at different reflector distances when $\ell=+1$ and $\ell=+3$ are multiplexed. B2B: the BER curve when there's no reflector and only a single OAM channel is transmitted.

DISCUSSION

Summarizing, we investigated the multipath-induced intra- and inter-channel crosstalk effects in a mm-wave communications link using OAM multiplexing. OAM channels with larger OAM ℓ values tend to have stronger intra-channel crosstalk because less power is received from the direct path and more power is reflected and received from the reflected path. The effect is caused by OAM beam divergence, as OAM beams with a larger ℓ diverge more and have less power in